energy&fuels

ARTICLE

pubs.acs.org/EF

Algae Polar Lipids Characterized by Online Liquid Chromatography Coupled with Hybrid Linear Quadrupole Ion Trap/Fourier Transform Ion Cyclotron Resonance Mass Spectrometry

Huan He,[†] Ryan P. Rodgers,[†,‡] Alan G. Marshall,[*,†,‡] and Chang Samuel Hsu[*,§]

[†]National High Magnetic Field Laboratory, Florida State University, 1800 East Paul Dirac Drive, Tallahassee, Florida 32310, United States

[‡]Department of Chemistry and Biochemistry, Florida State University, 95 Chieftain Way, Tallahassee, Florida 32306, United States

[§]Future Fuels Institute, Florida State University, Tallahassee, Florida 32310, United States

Supporting Information

ABSTRACT: We report the first application of online LC-MS (liquid chromatography−mass spectrometry) characterization of algae polar lipids by nanoscale high-performance liquid chromatography followed by electrospray ionization and mass analysis with a linear ion trap (LTQ) coupled with 14.5 T Fourier transform ion cyclotron resonance mass spectrometry (FT-ICR MS). Ultrahigh FT-ICR mass resolution provides highly accurate mass measurement and resolves monoisotopic peaks from interfering components for unique determination of lipid elemental compositions. We establish the polar lipid profile of fatty acids, glycolipids, phospholipids, and betaine lipids for a green algae, *Nannochloropsis oculata*, which is highly prized for its oils suitable for biodiesel production. Lipid headgroup and fatty acid identification is based on accurate mass measured by the FT-ICR MS and collision-induced dissociation (CID) MS/MS in the LTQ. Unequivocal lipid composition is further confirmed from isotopic fine structure at baseline resolution—achievable only with ultrahigh resolution FT-ICR MS.

INTRODUCTION

Transportation fuels have overwhelmingly been obtained from fossil resources. Because of dwindling supplies and increasing evidence of carbon dioxide as a main culprit for global warming, fuels from biological resources have been explored and have achieved some success. First generation biofuels are produced from food sources, such as vegetable oils, starch, and sugar.[1,2] To abate the competition with food sources, second generation biofuels are produced from nonfood sources, such as lignocellulosic biomass.[1,2] Algae, specifically microalgae, are considered as third generation biofuel feedstocks designed for fuel production as an "energy crop".[3] The use of marine algae would further reduce the competition for land and freshwater.

The current focus of third generation algae biofuel research is to discover new algae strains of high oil yield and to genetically modify algae to improve the intrinsic oil yield and growth rate. Genetic modification and external stimuli (e.g., nitrogen starvation) profoundly influence lipid biosynthetic and metabolic pathways. The long-term goal is to generate algae lipid fingerprints that can be mapped to those pathways. The insights thus generated should have a major impact on the understanding of algae oil biosynthesis and thus help to guide future genetic modification and strain selection.

Algae contain four principal biochemical classes: carbohydrates (polysaccharides), proteins, nucleic acids, and lipids. Algae produce various types of polysaccharides that can be fermented to produce alcohols for fuels. Lipids are feedstocks for biodiesel fuel through trans-esterification processes. Proteins, on the other hand, can be developed into high value biochemicals by virtue of their amino acid composition of high nutritional quality.[4]

The lipid content of microalgae is strongly influenced by growth conditions such as the effects of temperature and nitrogen content of *Nannochloropsis oculata* and *Chlorella vulgaris* for biodiesel production.[5] However, there is evidence of a negative relationship between growth rate and lipid content for naturally occurring algae. Hence, high lipid yield alone cannot be used as the only criterion for optimal growth conditions.[4]

Despite massive efforts on the development of biofuels from microalgae, the analysis of algae strains at the molecular level is woefully incomplete. Algae lipid analysis is especially relevant to prospective biodiesel and jet fuel production. We focus initially on *Nannochloropsis oculata* (green algae) because of its relatively high oil yield (40−60%).[6] Most prior lipid characterization methods are bulk or indirect analyses and cannot resolve and identify intact molecular structures.[7,8] Here, we combine online liquid chromatography (LC) with electrospray ionization Fourier transform ion cyclotron resonance mass spectrometry[9] (ESI FT-ICR MS) and tandem mass spectrometry (MS/MS) to resolve and identify lipid elemental compositions, $C_cH_hN_nO_oP_pS_s$, head groups, fatty acid chain lengths, and unsaturation of polar lipids from green algae, as a first step in the molecular level characterization of wild type and genetically engineered (mutant) algae[7,10] of improved growth rate and lipid yield for the production of algal fuels.[11]

Received: July 20, 2011
Revised: September 12, 2011
Published: September 26, 2011

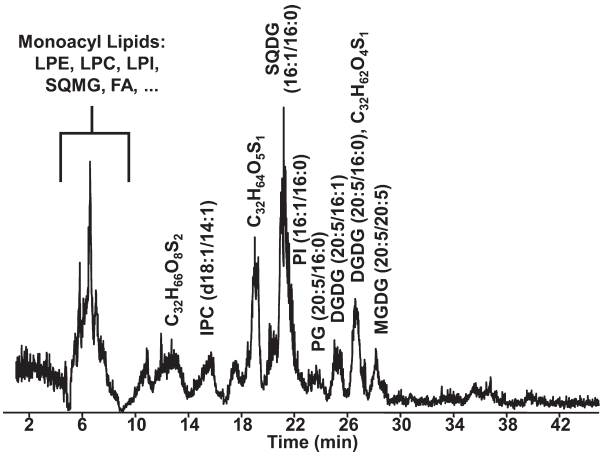

Figure 1. NanoLC-MS total ion chromatogram (TIC) showing representative algae polar lipids.

METHODS

Lipid Extraction. Algae polar lipids were extracted with a modified protocol for mammalian cells.[12] A green algae (*Nannochloropsis oculata*, UTEX, Austin, TX) suspension in 1 mL of Erdschreiber's medium[13] was centrifuged to remove supernatant; the residual pellet was lyophilized; and 0.4 mL of isopropanol (IPA) was added. After sonication for 5 min, 0.4 mL of chloroform was added, followed by another 5 min of sonication. The mixture was incubated at 48 °C, in a water bath, overnight. After centrifugation and the removal of the supernatant, 0.4 mL of 1:1 (v/v) $CH_3OH/CHCl_3$ was added to the residue, and the mixture was sonicated for 5 min before centrifugation to remove supernatant. The above step was repeated one more time, and the combined supernatant was dried. The dried lipid extract was taken up in 0.4 mL of 3:2 (v/v) H_2O/CH_3OH plus 60 μL of $CHCl_3$. After phase separation, the upper layer containing polar lipids and lower layer with nonpolar lipids were collected, dried, and stored at −80 °C.

Nano-Liquid Chromatography−Mass Spectrometry (nLC-MS). The polar lipid fraction was redissolved in 20:80 H_2O/CH_3OH containing 10 mM ammonium acetate (NH_4OAc) for subsequent nLC-MS analysis with an Eksigent (Dublin, CA) nanoLC-1D system. A phenylhexyl stationary phase (Phenomenex, Torrance, CA) was selected for its dual selectivity: namely, $\pi-\pi$ stacking interaction and reduced hydrophobic−hydrophobic interactions between the stationary phase and the analytes. The column (75 μm i.d. × 5 cm length) was custom-packed by New Objective (Woburn, MA). For gradient elution, solution A contained 98% H_2O, 2% CH_3OH, and 10 mM NH_4OAc and solution B contained 2% H_2O, 98% CH_3OH, and 10 mM NH_4OAc, with a gradient from 80% to 98% B in 30 min, at a flow rate of 400 nL/min. The LC effluent was subjected to negative-ion electrospray ionization (ESI) at −1.7 kV applied to the precolumn union, and detected online with a hybrid linear ion trap quadrupole (LTQ)/14.5 T Fourier transform ion cyclotron resonance (FT-ICR) mass spectrometer.[14] Three million target ions were collected in LTQ with automatic gain control (AGC)[15] before transfer to the ICR cell (55 mm i.d.) through octopole ion guides (2.2 MHz, 250 V_{p-p}). In the ICR cell, ions were SWIFT[16] excited with an m/z range from 176 to 10 200. FT-ICR MS data was acquired at a mass resolving power ($m/\Delta m_{50\%}$, in which $\Delta m_{50\%}$ is a mass spectral peak full width at half-maximum peak height) of 200,000 at 400 Da with time domain acquisition period of 767 ms. Calmix (Thermo Fisher, San Jose, CA) was used for external calibration.[17,18] Mass spectral data were analyzed with commercial software (Xcalibur, Thermo Fisher, San Jose, CA). Structural assignment was based on the accurate mass of the pseudomolecular ion $[M-H]^-$ for negative ESI FT-ICR MS and corresponding fragment ions detected by collision-induced dissociation (CID) under nitrogen (25% normalized collision energy) in the LTQ. Triplicate samples yielded average values and standard deviations of signal magnitude.

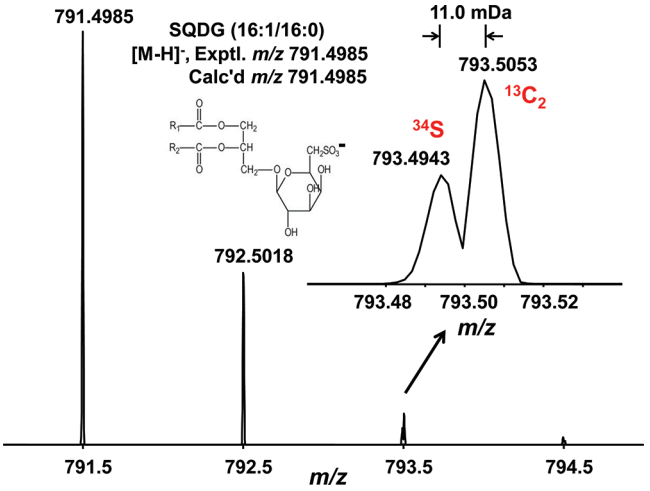

Figure 2. Isotopic distribution for the deprotonated molecular ion ($[M-H]^-$) of SQDG (16:1/16:0). The inset shows the ^{34}S and $^{13}C_2$ doublet. The observed mass difference between species differing by ^{34}S vs ^{32}S matches perfectly with the calculated value of 1.9958 Da. The observed abundance of ^{34}S relative to ^{32}S also matches the theoretical value of 4.2%. Thus, the sulfur content of the lipid species is confirmed.

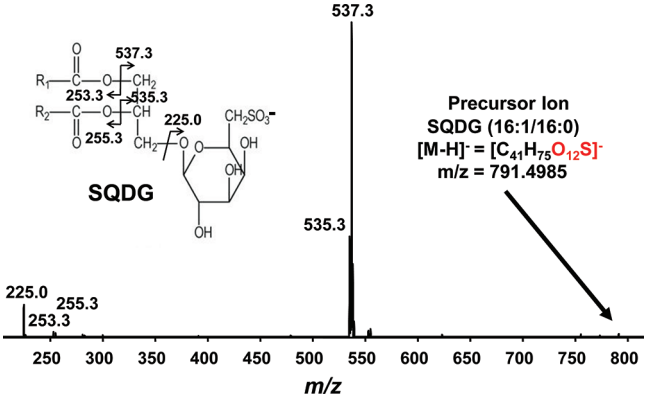

Figure 3. LTQ collision-induced dissociation (CID) product ion mass spectrum of the deprotonated molecular ion ($[M-H]^-$, 791.4985 Da) from a representative sulfoquinovosyldiacylglycerol (SQDG) (16:1/16:0). Note the characteristic 225.0 Da fragment ion at 225.0 Da, characteristic of the sulfoquinovosyl group.

RESULTS AND DISCUSSION

HPLC to Address Concentration Dynamic Range. Direct infusion of the polar lipid fraction of algae yields only nonlipid signals. Thus, LC separation prior to MS analysis is essential for lipid characterization by MS. Nano-LC requires only 2.4 μg dry

dx.doi.org/10.1021/ef201061j |*Energy Fuels* 2011, 25, 4770–4775

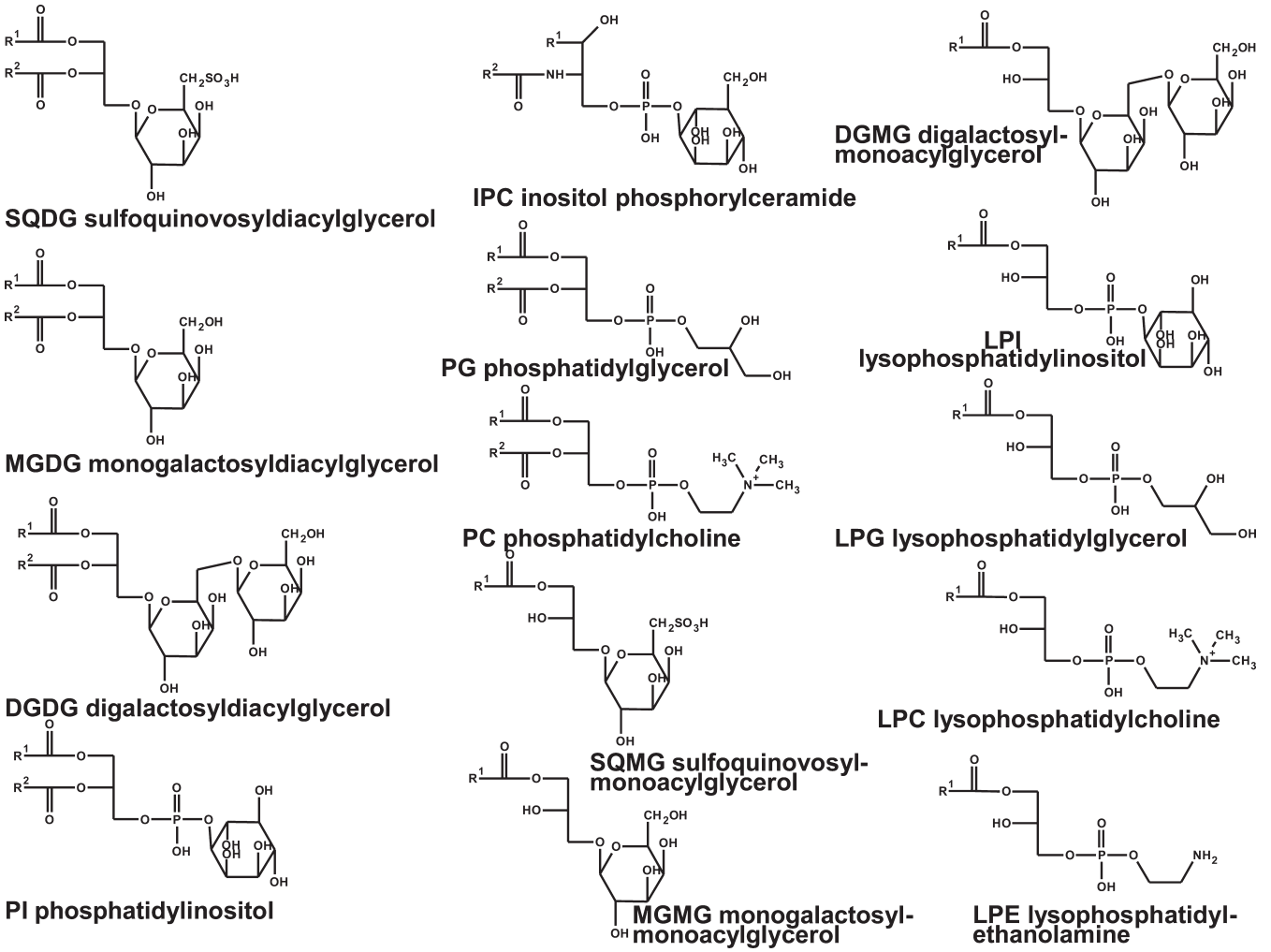

Figure 4. Representative algae lipids identified from *Nannochloropsis oculata*.

algae for each nLC-MS experiment. Two major fractions, monoacyl and diacyl lipids, are well separated under our LC conditions (see Figure 1). LC separation enables the MS analysis for a lipid mixture of high dynamic range and increases the number of detected lipids. We have identified nearly 200 unique lipid species (not counting various adducts) with a dynamic range greater than 20 000:1 (Table 1 in the Supporting Information).

Elemental Composition from Molecular Ion Accurate Mass Measurement. The structure of individual lipid species is determined by accurate mass (typically less than 500 ppb mass measurement error) of each pseudomolecular ion by FT-ICR MS and LTQ CID mass spectrum. For example, negative ESI FT-ICR MS of sulfoquinovosyldiacylglycerol (SQDG) yields a deprotonated molecular ion of 791.4985 Da, whose elemental composition may be uniquely assigned as $C_{41}H_{76}O_{12}S$ (Figure 2). That elemental composition is further confirmed by the resolution of two heavy isotopic forms containing ^{34}S or $^{13}C_2$ at 793.4943 Da ($C_{41}H_{76}O_{12}{}^{34}S$) and 793.5053 Da ($^{13}C_2C_{39}H_{76}O_{12}S$) (Figure 2 inset).

Collision-Induced Dissociation MS/MS. The structure of SQDG was determined by Collision-Induced Dissociation (CID) MS/MS of the deprotonated molecular ion (Figure 3). The most abundant product ion (537 Da) results from the loss of a singly unsaturated-C_{16} carboxyl group. Another at 535 Da is the result of losing a saturated-C_{16} carboxyl group. Based on the higher signal magnitude for ions of 537 Da relative to ions of 535 Da, we are able to assign the 16:1 fatty acid at the *sn*-1

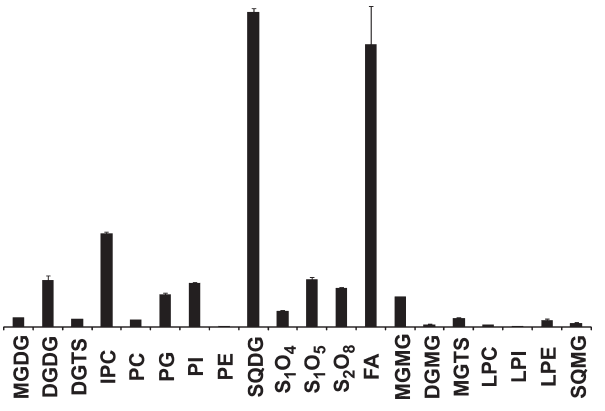

Figure 5. Relative mass spectral peak magnitudes for various identified lipid classes. Each entry represents the sum of the signal magnitudes, irrespective of the number of fatty acid alkyl carbons and double bonds. Each error bar represents the standard deviation from three analytical replicates.

dx.doi.org/10.1021/ef201061j |*Energy Fuels* 2011, 25, 4770–4775

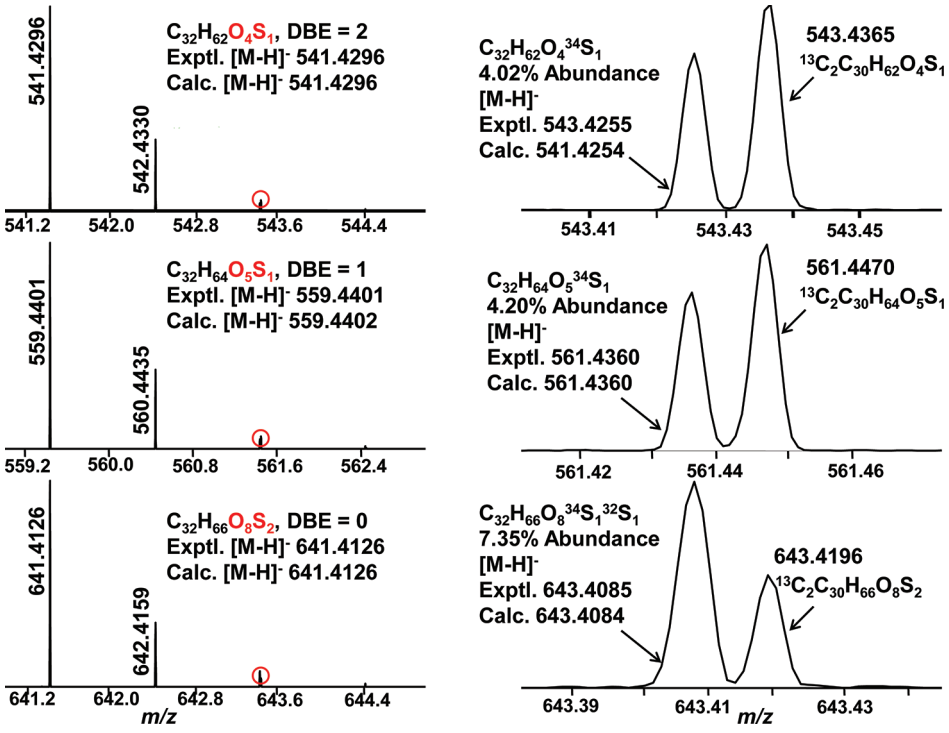

Figure 6. Deprotonated molecular ions of $C_{32}H_{62}O_4S$, $C_{32}H_{64}O_5S$, and $C_{32}H_{66}O_8S_2$ detected by online LC FT-ICR MS. Left: isotopic distribution. Right: near-baseline resolution of species differing by ^{34}S vs $^{13}C_2$.

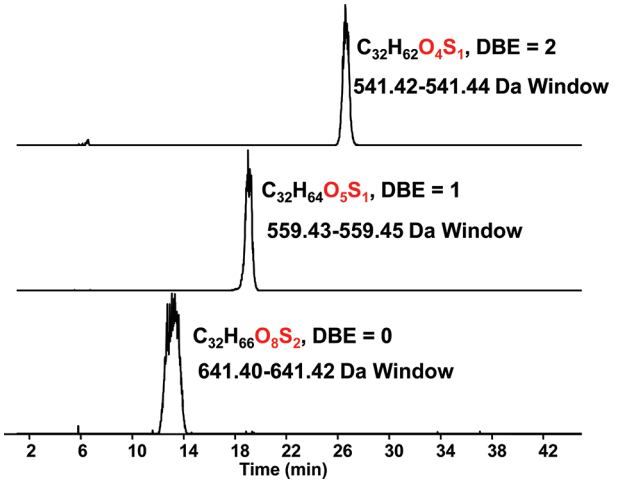

Figure 7. LC selected ion chromatograms for $C_{32}H_{62}O_4S$, $C_{32}H_{64}O_5S$, and $C_{32}H_{66}O_8S_2$. The retention time order, $C_{32}H_{62}O_4S$ > $C_{32}H_{64}O_5S$ > $C_{32}H_{66}O_8S_2$, corresponds to the polarity order, $C_{32}H_{62}O_4S$ < $C_{32}H_{64}O_5S$ < $C_{32}H_{66}O_8S_2$.

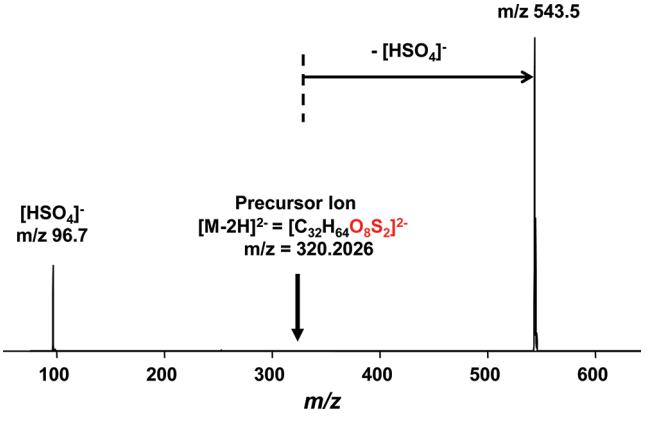

Figure 8. CID product ion mass spectrum of $[M - 2H]^{2-}$ from $C_{32}H_{66}O_8S_2$ by LTQ CID, characterized by the bisulfate fragment ion (96.7 Da) and a loss of bisulfate from the deprotonated molecular ion (543.5 Da).

position and the 16:0 fatty acid at the *sn*-2 position.[19] The presence of ions of 225 Da confirms the sulfoquinovosyl group.

In this way, we identify sulfoquinovosyldiacylglycerol (SQDG), digalactosyldiacylglycerol (DGDG), monogalactosyldiacylglycerol (MGDG), inositol phosphorylceramide (IPC), phosphatidylinositol (PI), phosphatidylglycerol (PG), diacylglyceryl-*N*,*N*,*N*-trimethylhomoserine (DGTS), phosphatidylcholine (PC), phosphatidylethanolamine (PE), fatty acids (FA), and lyso forms of the diacylglycerol lipids; structures are shown in Figure 4, and the relative ion abundances are shown in Figure 5. SQDG, a lipid mainly found in chloroplasts, is particularly prominent, as are free fatty acids. Two chloroplast membrane glycolipids, MGDG and DGDG, are also identified. The betaine lipid, DGTS, has been hypothesized to transfer fatty acid from the cytoplasm to chloroplast. We identify four types of phospholipids, including PI, PG, PC, and PE. Unlike diacylglycerol lipids, IPC contains a ceramide linkage. Ceramide and inositol groups are each linked to a phosphate group. Monoacylglycerol lipids are typically at lower concentration than diacylglycerol lipids.

Sulfur-Containing Lipids. In addition to lipid species previously reported in the literature, we identified a series of novel polar lipids containing O_4S_1, O_5S_1 and O_8S_2. Figure 6 shows

dx.doi.org/10.1021/ef201061j |*Energy Fuels* 2011, 25, 4770–4775

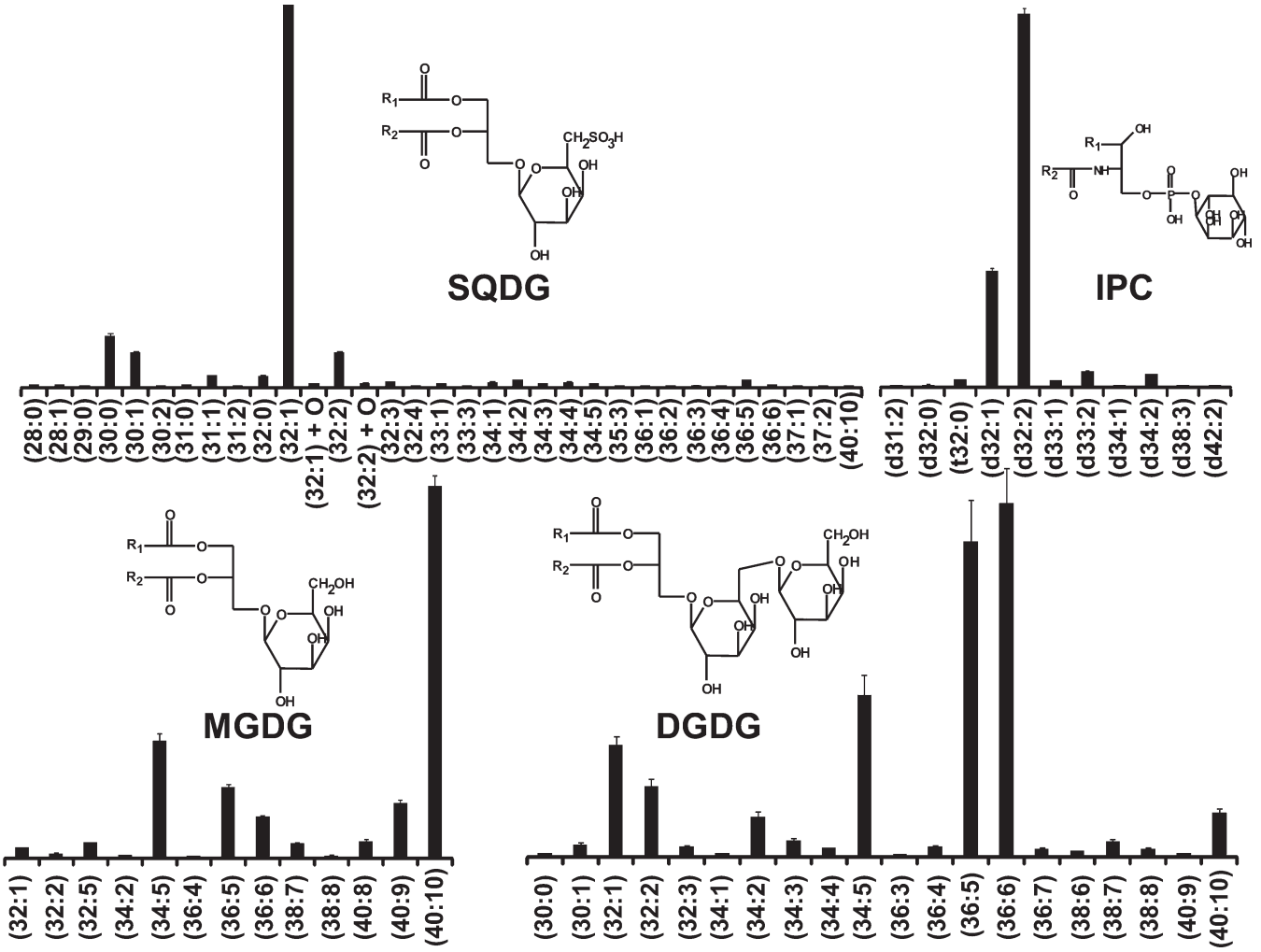

Figure 9. Relative signal magnitudes of lipid isoforms (lipids with the same polar headgroup but different hydrophobic tails) for different lipid classes. The dominant SQDG isoform (32:1) is composed mainly of the (16:1/16:0) diacyl group. A minor component of SQDG contains PUFA. The principal MGDG isoform (40:10) mainly contains the (20:5/20:5) diacyl group. A minor MGDG component contains saturated fatty acid. DGDG. The major DGDG isoforms (36:6) and (36:5) mainly comprise the (16:1/20:5) and (16:0/20:5) diacyl groups. The primary IPC isoform (d36:2) contains 2 hydroxyl groups, 32 total carbons, and 2 double bonds in the ceramide tails. Additional chemical labeling and/or MS/MS stage(s) would be needed to determine the dominant fatty acid and sphingosine of the ceramide tail.

FT-ICR MS of three representative lipid species from each group, $C_{32}H_{62}O_4S$, $C_{32}H_{64}O_5S$, and $C_{32}H_{66}O_8S_2$. Elemental composition is established from ultrahigh mass accuracy for the monoisotopic ion (Figure 6, left) and further confirmed from the isotopic fine structure (Figure 6, right). Even with the relatively short ICR time-domain data acquisition period (767 ms, limited by online LC flow rate), we are able to separate ions differing in composition by ^{34}S vs $^{13}C_2$ with near-baseline resolution. Moreover, the abundance ratio of ions differing in composition by ^{34}S vs ^{32}S further confirms the number of sulfur atoms. The natural fractional abundance of ^{34}S relative to ^{32}S is 4.2%,[20] a value closely approached experimentally for $C_{32}H_{62}O_4S$ and $C_{32}H_{64}O_5S$ (Figure 6, upper and middle right) The presence of two sulfur atoms in $C_{32}H_{66}O_8S_2$ is confirmed by the observed ^{34}S-containing ion relative abundance of ~8% (Figure 6, bottom right). Based on the high abundance as negative ions, it is likely that the sulfur is present in the form of sulfate.

Figure 7 shows the LC elution profiles for the most abundant lipid from each group, $C_{32}H_{62}O_4S$, $C_{32}H_{64}O_5S$, and $C_{32}H_{66}O_8S_2$. Because phenylhexyl stationary phase behaves like a conventional reversed-phase resin, we infer a polarity order, $C_{32}H_{62}O_4S$ < $C_{32}H_{64}O_5S$ < $C_{32}H_{66}O_8S_2$. Also, from the double bond equivalence, DBE, computed from the elemental composition, $C_cH_hN_n$... (DBE = $c - {}^{h}/_{2} + {}^{n}/_{2} + 1$ = number of rings plus double bonds to carbon) we postulate that $C_{32}H_{62}O_4S$ has one more double bond than $C_{32}H_{64}O_5S$. Similarly, $C_{32}H_{64}O_5S$ has one more double bond than $C_{32}H_{66}O_8S_2$. The presence of a sulfate group is further corroborated by the CID product ion mass spectrum of $[M - 2H]^{2-}$ from $C_{32}H_{66}O_8S_2$, shown in Figure 8. Because the sulfate group is highly labile, the dominant fragment ions are the bisulfate ion, $[HSO_4]^-$ (96.7 Da) and a loss of bisulfate (97 Da) from the deprotonated molecular ion (543.5 Da).

Polyunsaturated Fatty Acid Chains. *Nannochloropsis oculata* is a rich source of highly polyunsaturated fatty acids (PUFA), including eicosahexaenoic acid (EHA, 20:6), eicosapentaenoic acid (EPA, 20:5), and eicosatetraenoic acid, (ETA, 20:4) (Table 1 in the Supporting Information). Of great interest is the variation

of the preferred diacylglycerol backbone for different lipid species. For example, SQDG prefers (16:1/16:0) (Figure 9), whereas MGDG and DGDG prefer PUFA. The most abundant MGDG contains (20:5/20:5) fatty acids (Figure 9) whereas the dominant DGDG contains (16:0/20:5) and (16:1/20:5) (Figure 9). That variation suggests different enzymatic pathways in fatty acid utilization. For the ceramide-containing lipid, IPC, we do not observe any PUFA-containing isoforms. The major isomer contains 2 hydroxyls, 32 total carbons, and 2 double bonds in its ceramide tail (d32:2) (Figure 9). The fatty acid chain length and the number of double bonds can profoundly affect the properties of lipid bilayers. Thus, such diversity in preferred lipid isoforms for different lipid species suggests not only complex lipid biosynthesis/metabolism networks but also different functions/localization of different lipid species.

CONCLUSION

Identification of algae polar lipids requires a combination of extraction (to isolate the lipid fraction), HPLC (to overcome the high dynamic concentration range), ultrahigh resolution FT-ICR MS (for unique elemental composition), and MS/MS (to identify polar headgroups as well as fatty acid chain lengths and degrees of unsaturation). Lipid elemental composition is unequivocally assigned from accurate mass measurement of the molecular ion and from isotopic fine structure at baseline resolution, possible only with ultrahigh resolution FT-ICR MS,[9] as previously demonstrated by resolution and elemental composition assignment of tens of thousands of constituents of petroleum crude oil.[21,22] Recent improvements in FT-ICR mass resolution and speed of data acquisition,[23] mass calibration and accuracy,[24] and higher magnetic field[14] further extend its reliability and range.

ASSOCIATED CONTENT

Supporting Information. Supplementary Table 1: Polar lipids identified from *Nannochloropsis oculata*. This material is available free of charge via the Internet at http://pubs.acs.org.

AUTHOR INFORMATION

Corresponding Author

*E-mail: hsu@magnet.fsu.edu; marshall@magnet.fsu.edu.

ACKNOWLEDGMENT

This work was supported by the National Science Foundation Division of Materials Research through DMR-0654118 and the State of Florida.

REFERENCES

(1) Noweck, K. *Hydrocarbon Process.* **2007**, *86*, 83–84.
(2) Naik, S. N.; Goud, V. V.; Rout, P. K.; Dalai, A. K. *Renewable Sustainable Energy Rev.* **2010**, *14*, 578–597.
(3) Singh, A.; Nigam, P. S.; Murphy, J. D. *Bioresour. Technol.* **2011**, *102*, 10–16.
(4) Williams, P. J. L.; Laurens, L. M. L. *Energy Environ. Sci.* **2010**, *3*, 554–590.
(5) Converti, A.; Casazza, A. A.; Ortiz, E. Y.; Perego, P.; Del Borghi, M. *Chem. Eng. Process* **2009**, *48*, 1146–1151.
(6) *Algae Oil Yields*. Available online: http://www.oilgae.com/algae/oil/yield/yield.html.
(7) Lee, M. Y.; Min, B. S.; Chang, C. S.; Jin, E. *Mar. Biotechnol.* **2006**, *8*, 238–245.
(8) Su, C.-H.; Fu, C.-C.; Chang, T.-C.; Nair, G. R.; Ye, J. L. *Biotechnol. Bioeng.* **2007**, *99*, 1034–1039.
(9) Marshall, A. G.; Hendrickson, C. L.; Jackson, G. S. *Mass Spectrom. Rev.* **1998**, *17*, 1–35.
(10) Radakovits, R.; Jinkerson, R. E.; Darzins, A.; Posewitz, M. C. *Eukaryotic Cell* **2010**, *9*, 486–501.
(11) Hsu, C. S.; He, H.; Lu, J.; Lobodin, V. V.; Emmett, M. R.; Marshall, A. G.*59th American Society for Mass Spectrometry Conference on Mass Spectrometry and Allied Topics*, Denver, CO, June 4—9, 2011.
(12) He, H.; Conrad, C. A.; Nilsson, C. L.; Ji, Y. J.; Schaub, T. M.; Marshall, A. G.; Emmett, M. R. *Anal. Chem.* **2007**, *79*, 8423–8430.
(13) *University of Texas Austin UTEX Culture Collection of Algae*. Available online: http://www.sbs.utexas.edu/utex/default.aspx.
(14) Schaub, T. M.; Hendrickson, C. L.; Horning, S.; Quinn, J. P.; Senko, M. W.; Marshall, A. G. *Anal. Chem.* **2008**, *80*, 3985–3990.
(15) Schwartz, J. C.; Senko, M. W.; Syka, J. E. P. *J. Am. Soc. Mass Spectrom.* **2002**, *13*, 659–669.
(16) Guan, S.; Marshall, A. G. *Anal. Chem.* **1993**, *65*, 1288–1294.
(17) Ledford, E. B., Jr.; Rempel, D. L.; Gross, M. L. *Anal. Chem.* **1984**, *56*, 2744–2748.
(18) Shi, S. D.-H.; Drader, J. J.; Freitas, M. A.; Hendrickson, C. L.; Marshall, A. G. *Int. J. Mass Spectrom.* **2000**, *195/196*, 591–598.
(19) Murphy, R. C. *Mass Spectrometry of Phospholipids: Tables of Molecular and Product Ions*; Illuminati Press: Denver, CO, 2002.
(20) National Institute of Standards and Technology. *Atomic Weights and Isotopic Compositions*. Available online: http://physics.nist.gov/cgi-bin/Compositions/stand_alone.pl?ele=&ascii=html&isotype=all.
(21) Marshall, A. G.; Rodgers, R. P. *Proc. Natl. Acad. U.S.A.* **2008**, *105*, 18090–18095.
(22) Hsu, C. S.; Hendrickson, C. L.; Rodgers, R. P.; McKenna, A. M.; Marshall, A. G. *J. Mass Spectrom.* **2011**, *46*, 337–343.
(23) Xian, F.; Hendrickson, C. L.; Blakney, G. T.; Beu, S. C.; Marshall, A. G. *Anal. Chem.* **2010**, *82*, 8807–8812.
(24) Savory, J. J.; Kaiser, N. K.; McKenna, A. M.; Xian, F.; Blakney, G. T.; Rodgers, R. P.; Hendrickson, C. L.; Marshall, A. G. *Anal. Chem.* **2011**, *83*, 1732–1736.